Journal of Catalysis 275 (2010) 181–185

Contents lists available at ScienceDirect

Journal of Catalysis

journal homepage: www.elsevier.com/locate/jcat

Research Note

Ceria reoxidation by CO_2: A model study

T. Staudt[a], Y. Lykhach[a,*], N. Tsud[b], T. Skála[c], K.C. Prince[c], V. Matolín[b,c], J. Libuda[a,d]

[a] *Lehrstuhl für Physikalische Chemie II, Department Chemie und Pharmazie, Friedrich-Alexander-Universität Erlangen-Nürnberg, Egerlandstr. 3, 91058 Erlangen, Germany*
[b] *Charles University, Faculty of Mathematics and Physics, Department of Surface and Plasma Science, V Holešovičkách 2, 1800 Prague 8, Czech Republic*
[c] *Sincrotrone Trieste SCpA, Strada Statale 14, km 163.5, 34149 Basovizza-Trieste, Italy*
[d] *Erlangen Catalysis Resource Center, Friedrich-Alexander-Universität Erlangen-Nürnberg, Egerlandstr. 3, 91058 Erlangen, Germany*

ARTICLE INFO

Article history:
Received 31 May 2010
Revised 20 July 2010
Accepted 24 July 2010

Keywords:
Ceria
Carbon dioxide
Model catalyst
Heterogeneous catalysis
Resonant photoelectron spectroscopy

ABSTRACT

The activation of CO_2 on ceria-based catalysts opens chemical routes to the use of CO_2 as an oxidizing agent. Toward a better understanding of the underlying surface reactions, we have performed a model study on well-defined CeO_{2-x} thin films on Cu(1 1 1) under ultra-high-vacuum conditions. Resonant photoelectron spectroscopy is used as a highly sensitive tool to monitor changes in the oxidation state of cerium as a function of CO_2 exposure and thermal treatment. It is shown that partial reoxidation of CeO_{2-x} by CO_2 occurs with high reaction probabilities (i) even at temperatures as low as room temperature, (ii) on pure CeO_{2-x} in the complete absence of any noble metal co-catalysts, and (iii) in the absence of surface hydroxyl groups or water. In contrast to previous studies on ceria powders, the findings clearly demonstrate the high activity of pure hydroxyl- and metal-free ceria surfaces for CO_2 activation, even at low reaction temperatures.

1. Introduction

The rare earth oxide ceria (CeO_2) and ceria-containing mixed oxides exhibit unique properties in numerous heterogeneously catalyzed processes [1]. Many of these properties are related to the remarkable capability of cerium oxide to store and release oxygen, a process that is accompanied by reversible transformation between two oxidation states of Ce, Ce^{4+} and Ce^{3+}. Moreover, it has been found that CO_2 activation is possible via several routes, specifically, rapid formation of carbonate [2–4], carboxylate [2–4], and bicarbonate [4] species on partially reduced CeO_{2-x}, as well as the direct dissociation of CO_2 on metal-loaded ceria [5–7]. The attractive possibility of using CO_2 as an oxidizing agent opens a route to technically important reactions such as dry reforming of methane or partial oxidation of hydrocarbons (see, e.g., [8–12]).

The underlying chemistry is poorly understood at the molecular level, and contradictory results have been published. For instance, an ambiguity concerns CO_2 activation via direct dissociation of the molecule to CO and oxygen. Bradford and Vannice [13] described the mechanism of CO_2 dissociation as a two-step process that involves formation of carbonates followed by interaction with hydrogen. The hydrogen could be delivered to the carbonate site via spillover upon decomposition of hydrocarbons. For oxides, the presence of hydrogen may lead to the formation of surface hydroxyl groups. Reaction of carbonates with hydroxyl groups can yield CO and water.

In contrast to the mechanism described above, the direct dissociation of CO_2, without hydrogen/hydroxyl groups, was observed on noble-metal-loaded ceria and ceria–zirconia surfaces, mainly using Pd and Pt as active metals [5–7]. Therefore, it has been proposed that metal oxide interaction or boundary regions play a critical role in CO_2 dissociation [5,6]. Demoulin et al., however, questioned the role of intimate metal/oxide interaction in CO_2 activation [7]. Makkee and co-workers [14] demonstrated an isotopic oxygen exchange between CO_2 and ceria on both Pt/CeO_2 and CeO_2 samples. Moreover, Otsuka et al. reported the reoxidation of reduced ceria by CO_2, accompanied by the formation of pure CO [15]. However, the activation of CO_2 occurred at elevated temperatures, 473 K or higher, similarly to nearly all other studies on CO_2 activation on ceria. There is only one experimental investigation in which CO_2 activation via dissociation at room temperature has been reported: In an older study, White and co-workers studied the interaction of CO_2 with a Pt/ceria catalyst by FT-IR and X-ray photoelectron spectroscopy [5]. They found that CO is formed by decomposition of CO_2 on partially reduced Pt/ceria catalysts, whereas on fully preoxidized catalysts no reactivity is observed. Again, the authors attributed the activity to CO_2 dissociation occurring at the metal/oxide boundary.

To obtain more clarity on the mechanism of CO_2 activation on ceria, we have performed a model study using a surface science approach. Contradicting several of the above-mentioned hypotheses, we show that reoxidation of ceria by CO_2 actually requires neither

---

[*] Corresponding author. Fax: +49 9131 8528867.
E-mail address: yaroslava.lykhach@chemie.uni-erlangen.de (Y. Lykhach).

0021-9517/$ - see front matter © 2010 Elsevier Inc. All rights reserved.
doi:10.1016/j.jcat.2010.07.032

the presence of a noble metal nor the presence of surface hydroxyl groups. In fact, the atomically clean and strongly reduced ceria surface exhibits high intrinsic activity toward CO_2, leading to partial reoxidation even at room temperature.

Our experimental approach involves the use of a ceria model catalyst under ultra-high-vacuum (UHV) conditions. This allows us to prepare contamination-free surfaces, which can be investigated using the full spectrum of surface science tools (see, e.g., [16,17]). In the present work we use an epitaxial $CeO_2(1\,1\,1)$ film as a model support, which is grown on a Cu(1 1 1) single-crystal surface. For details on the preparation procedure, we refer to the literature [18–20]. Immediately after preparation, we obtain a well-ordered and fully stoichiometric film, with a concentration of Ce^{3+} below the detection limit of conventional XPS [21]. The nanostructure of the film exhibits a stepped surface, with top terraces mostly covered with small oxide aggregates. The step heights were 3.1 and 6.3 Å, corresponding to monolayer (particularly an O–Ce–O trilayer) and double-layer (two O–Ce–O trilayers) steps [20]. To prepare a partially reduced CeO_{2-x} surface, we follow a procedure previously described by Matolín et al. [22]. Briefly, the reduction procedure is based on the adsorption and subsequent thermal decomposition of methanol. After annealing to 700 K in UHV, we obtain a partially reduced dehydroxylated ceria surface. We use this model system to investigate the interaction and activation of CO_2.

2. Results and discussion

Changes of the oxidation state of Ce during the reaction can be monitored by conventional XPS following the characteristic Ce3*d* photoemission features of Ce^{3+} and Ce^{4+} (see, e.g., [1,21–24]). Thus, a primary indication of reoxidation of reduced ceria upon CO_2 adsorption at 300 K was observed [25]. However, the sensitivity of this method is comparatively poor and small changes in the concentration of Ce^{3+} are difficult to observe. Therefore, we use a synchrotron-radiation-based method that relies on the tunability of the photon energy ($h\nu$), namely resonant photoelectron spectroscopy (RPES). Indeed, RPES is among the most sensitive tools for the detection of changes in the oxidation state of ceria (see, e.g., [26–28] and references therein). Briefly, the method is based on measuring the valence bands at photon energies corresponding to the $4d \rightarrow 4f$ resonance either at Ce^{3+} or at Ce^{4+} centers. The two oxidation states of Ce differ with respect to the occupation of the 4*f* levels (Ce^{4+}: $4f^0$; Ce^{3+}: $4f^1$). In an indirect two-step photoemission process, a 4*d* electron is excited to a 4*f* level, followed by efficient decay via a Super–Coster–Kronig transition. Thus, for Ce^{3+}, the resonant PE process can be described by

$$4d^{10}4f^1 + h\nu \rightarrow 4d^9 4f^2 \rightarrow 4d^{10}4f^0 + e^-$$

with the final state appearing at a binding energy (BE) of 1.5 eV and showing a maximum resonance at $h\nu$ = 121.4 eV (see [27]). For Ce^{4+}, the resonant PE event is described by

$$4d^{10}4f^0 + h\nu \rightarrow 4d^9 4f^1 \rightarrow 4d^{10}4f^0 L + e^-$$

(*L* stands for a hole in the valence band), showing maximum resonant enhancement at $h\nu$ 124.8 eV, while the corresponding peak is located around 4 eV BE. Additionally, valence band spectra are measured at $h\nu$ = 115 eV, corresponding to an off-resonance condition.

The corresponding spectra for the fully stoichiometric $CeO_2(1\,1\,1)$ film are displayed in Fig. 1a. Indeed, we find that the resonant Ce^{3+} VB feature at 1.5 eV BE is hardly visible. This confirms the nearly perfect stoichiometry of the CeO_2 film on Cu(1 1 1) immediately after preparation. In Fig. 1b, the corresponding spectra are displayed after the reduction procedure using methanol has been applied (see Section 3 and [22] for details). Qualitatively, it is apparent that after reduction the resonant enhancement of the Ce^{4+} related emission (4 eV BE) decreases moderately, whereas we observe a very strong increase of the resonant enhancement of the Ce^{3+} emission (1.5 eV BE). In order to analyze the spectral changes in a more quantitative fashion we calculate the so-called resonant enhancement ratio (RER). This is done by first determining the individual resonant enhancements for Ce^{3+} (denoted as $D(Ce^{3+})$) and for Ce^{4+} ($D(Ce^{4+})$) as intensity differences between the corresponding spectra in- and off-resonance (compare [26,27]). The RER, calculated as $D(Ce^{3+})/D(Ce^{4+})$, directly reflects the Ce^{3+}/Ce^{4+} ion ratio. It is seen that the RER increases from 0.03 for the freshly prepared fully stoichiometric ceria film to a value of 4.1 after reduction. In order to determine the ceria stoichiometry from the RER values, we have fitted the Ce3*d* XP spectra of reduced CeO_{2-x} acquired during same experiment (see [21,23] for details). Although the sensitivity of conventional XPS with respect to determination of the Ce^{3+} concentration is much smaller than for RPES, an approximate calibration in terms of the ceria stoichiometry can be obtained. These estimated stoichiometries are given in the figures (see Fig. 2). It is found that after reduction the stoichiometry corresponds to a value of approximately $CeO_{1.79}$.

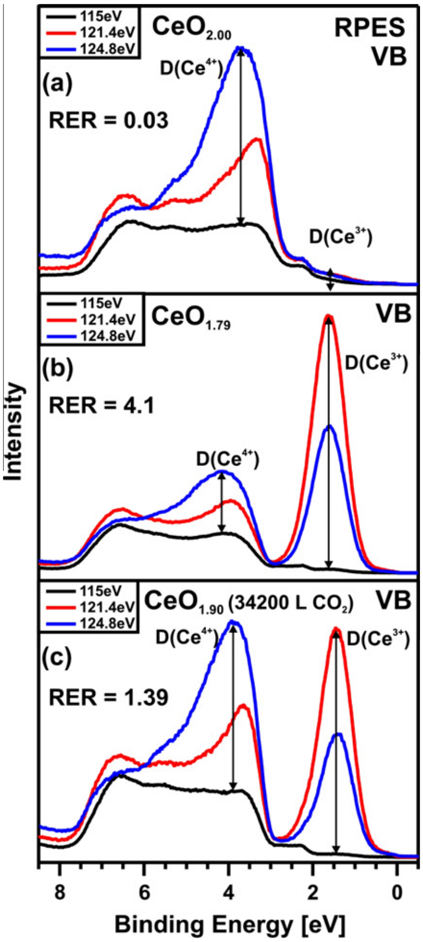

Fig. 1. Valence-band photoelectron spectra at different photon energies ($h\nu$) showing the resonant enhancement of Ce^{3+}- and Ce^{4+}-related features (Ce^{3+} resonance: $h\nu$ = 121.4 eV; Ce^{4+} resonance: $h\nu$ = 124.8 eV; off-resonance: 115 eV): (a) stoichiometric $CeO_2(1\,1\,1)$ film on Cu(1 1 1); (b) reduced ceria film (estimated stoichiometry $CeO_{1.79}$; see text for details) before CO_2 exposure; (c) reduced ceria film after partial reoxidation by CO_2 at 300 K (CO_2 dose: 34,200 L; estimated stoichiometry $CeO_{1.90}$).

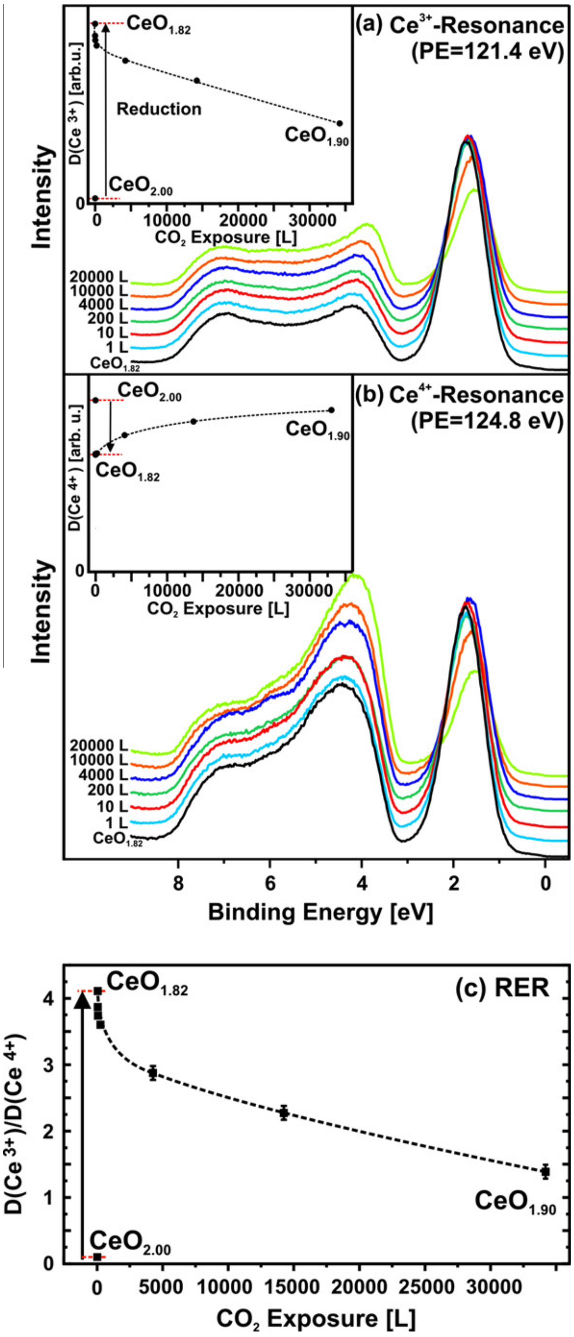

Fig. 2. Valence-band photoelectron spectra of the reduced ceria film on Cu(1 1 1) after exposure to different doses of CO_2 at 300 K: (a) valence band spectra at the Ce^{3+} resonance ($h\nu$ = 121.4 eV); the inset shows the Ce^{3+} resonant enhancement (see text for details); (b) valence band spectra at the Ce^{4+} resonance ($h\nu$ = 124.8 eV); the inset shows the Ce^{4+} resonant enhancement; (c) resonant enhancement ratio as a function of CO_2 exposure at 300 K. The estimated stoichiometries are also given (see text for details).

In the next step, we probe the interaction of CO_2 with the reduced ceria film. The surface is exposed to increasing doses of CO_2 at a surface temperature of 300 K (see Section 3 for details). The maximum total CO_2 dose applied was 34,200 L (1 L = Langmuir corresponds to a gas dose of 1.33×10^{-6} mbar × 1 s). After each dose, the RPE spectra, as well as C1*s*, Ce3*d*, and O1*s* core-level spectra were acquired using synchrotron and Al Kα radiation, respectively. The C1*s* spectra, measured by XPS and synchrotron radiation PES after each deposition step, revealed features at 290.1 eV BE and 287.2 eV (not shown). These findings are consistent with our previous study on the interaction of CO_2 with ceria and MgO-modified ceria by conventional XPS [25]. Tentatively, these features can be associated with surface carbonates (290.1 eV) and carboxylates (287.2 eV) on Ce^{3+} (see [25] and references therein). In the current experiment we found that the surface of the reduced ceria is saturated with mostly carboxylates after the adsorption of 1 L of CO_2.

In the present letter, we focus on the effect of reoxidation of the reduced ceria due to direct dissociation of CO_2 observed in RPES experiment. The corresponding VB spectra after an exposure to a total dose of 34,200 L CO_2 are shown in Fig. 1c. It is immediately evident that the relative intensity of the Ce^{3+}-resonance decreases dramatically upon CO_2 exposure. A more detailed analysis is displayed in Fig. 2. Sequences of VB spectra taken at 121.4 eV (Ce^{3+} resonance, Fig. 2a) and 124.8 eV (Ce^{4+} resonance, Fig. 2b) are shown together with the resonant enhancements for Ce^{3+} ($D(Ce^{3+})$, inset in Fig. 2a) and Ce^{4+} ($D(Ce^{4+})$, inset in Fig. 2b). In Fig. 2c the RER $D(Ce^{3+})/(D(Ce^{4+})$ is displayed as a function of CO_2 exposure. We observe that the RER decreases immediately upon CO_2 exposure. Starting from an initial value of 4.1, the RER decreases to a value of 3.7 at 11 L CO_2, and to a value of 1.4 at 34,200 L CO_2. Using the same calibration, based on the Ce3*d* XP spectra as mentioned above, we calculate a change in stoichiometry from initially $CeO_{1.79}$ to $CeO_{1.80}$ (11 L CO_2) and $CeO_{1.90}$ (34,200 L CO_2), respectively.

From these data, it is apparent that a substantial reoxidation of the reduced ceria film occurs upon CO_2 exposure at room temperature. Taking into account the CO_2 impingement rates and ceria ion density, we may even derive a rough estimate of the reaction probability: For the ideal CeO_2(1 1 1) film, we calculate a Ce ion density of 7.9×10^{14} cm^{-2} per ceria layer. If we assume that at room temperature reoxidation mainly affects the topmost ceria layer and taking into account that 1 L CO_2 corresponds to 3.0×10^{14} molecules cm^{-2}, we calculate an average reaction probability of approximately 3×10^{-3} for 11 L CO_2, which decreases to 9×10^{-6} for 34,200 L CO_2. This estimate shows that the reaction probability is quite large for the strongly reduced surface, but decreases rapidly as the reaction proceeds. We will come back to this point later.

Before, however, we analyze the thermal behavior of the ceria film after CO_2 treatment. Toward this aim, the sample was stepwise annealed up to a temperature of 700 K. The corresponding experimental data is displayed in Fig. 3a and b, respectively, together with the resonant enhancements $D(Ce^{3+})$ and $D(Ce^{4+})$ shown in the insets. The RE ratio $D(Ce^{3+})/(D(Ce^{4+})$ calculated from the above data is plotted in Fig. 3c.

We can clearly differentiate between two temperature regimes. At temperatures up to 500 K a moderate increase of the Ce^{3+} resonant enhancement is observed (RER = 1.9 at 500 K), together with an almost constant Ce^{4+} resonant enhancement signal. At temperatures of 550 K and above, a massive increase of the RER is found, which finally reaches a value of 3.6 at 700 K.

Analysis of the C1*s* spectra suggests that the most of the surface carbonates and carboxylates, formed upon CO_2 exposure, decompose upon annealing up to 550 K. This observation is consistent with a previous laboratory XPS study from our group [25]. Simple decomposition of surface carbonates under evolution of CO_2 is not expected to give rise to any significant change of the oxidation state of nearby ceria centers. However, is has been found that carbonate formation preferentially occurs at Ce^{3+} centers, leading to selective attenuation of photoemission signals from these sites [25]. Therefore, we attribute the slight increase in the resonant enhancement $D(Ce^{3+})$ to a decreasing attenuation of photoemission from Ce^{3+} sites due to decomposition of carbonates. This interpretation is consistent with the observation that the Ce^{4+} resonance remains nearly unaffected in this temperature range. At temperatures of 550 K and above, we observe an increase of the Ce^{3+}

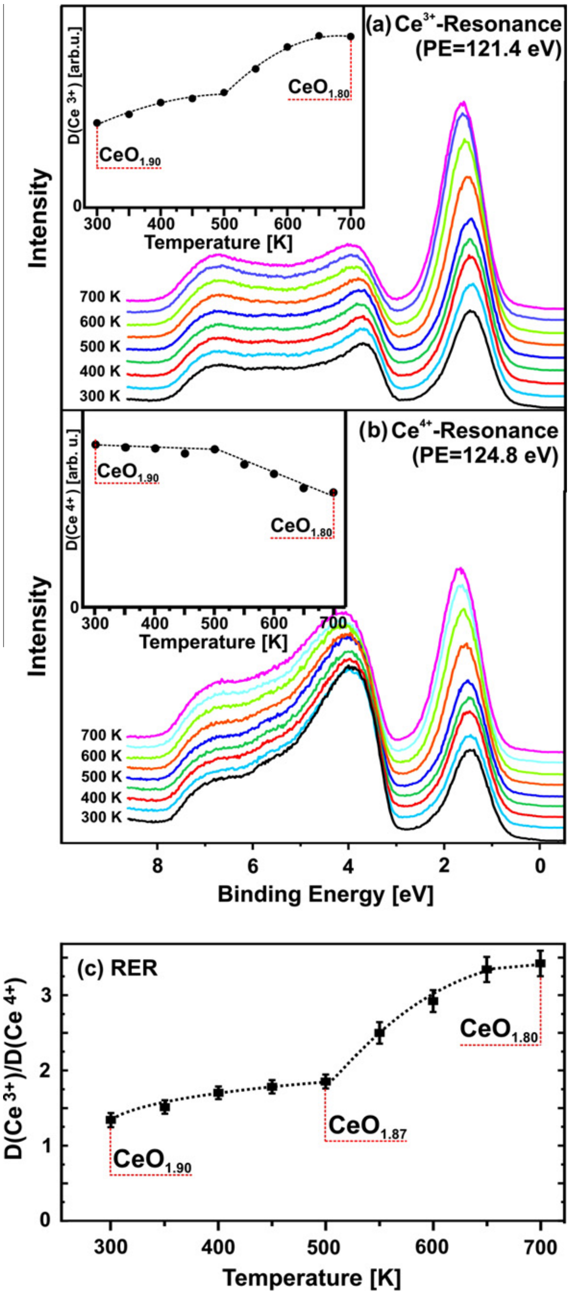

Fig. 3. Valence-band photoelectron spectra of ceria film, after reduction, partial reoxidation by CO_2, and after subsequent annealing to different temperatures: (a) valence band spectra at the Ce^{3+} resonance ($h\nu = 121.4$ eV); the inset shows the Ce^{3+} resonant enhancement; (b) valence band spectra at the Ce^{4+} resonance ($h\nu = 124.8$ eV); the inset shows the Ce^{4+} resonant enhancement; (c) resonant enhancement ratio as a function of annealing temperature. The estimated stoichiometries are also given (see text for details).

related resonant intensity enhancement together with a decrease of Ce^{4+} resonance. We attribute this effect to a genuine reduction of the ceria film as a result of a thermally induced loss of oxygen. The low threshold temperature for oxygen loss may be associated to the low degree of ordering obtained during the low temperature CO_2 reoxidation.

Our above described experiments reveal two important findings in the context of the present literature on the interaction of CO_2 with ceria-based catalysts: First, it is clearly shown that no noble metal component is required to facilitate CO_2 activation on ceria surfaces. In view of this observation, we may question previous hypotheses on the role of metal/oxide boundary sites for CO_2 activation [5,6]. Such sites may certainly facilitate additional reaction pathways, but clearly they are not a necessary precondition for CO_2 activation on ceria. The second conclusion concerns the role of surface OH groups or H_2O. The present experiments were performed on preannealed ceria films under UHV conditions, with no evidence for the presence of surface hydroxyl on these samples. Thus, we conclude that the reaction with surface hydroxyl is also not a mandatory step in CO_2 activation on ceria. In fact, it appears most likely that CO_2 can be activated at pure Ce^{3+} centers on pure and strongly reduced ceria. This intrinsic pathway to CO_2 decomposition is characterized by a low activation barrier, so that it can become highly efficient even at room temperature.

Certainly, this somewhat surprising conclusion deserves a more detailed discussion. First we may ask for the preconditions for CO_2 activation on ceria from a thermodynamic point of view. The reaction of CO_2 to CO and ½ O_2 is strongly endothermic, with a reaction enthalpy of +283 kJ mol^{-1} at standard temperature and pressure. Thus, the reaction will become feasible only if sufficient energy is provided by annealing of oxygen vacancies. Recent density functional theory (DFT) calculations yielded a value of 2.65 eV (256 kJ mol^{-1}) for the formation of oxygen vacancies (under release of ½ O_2) on ideal CeO_2(1 1 1) [29]. The difference is small, but may suggest that low concentrations of oxygen vacancies on CeO_2(1 1 1) will not facilitate spontaneous CO_2 activation. The situation may change, however, if we go to higher vacancy densities or strongly reduced nanoparticles, enforcing energetically less favorable vacancy configurations. Recent calculations, both on CeO_2(1 1 1) [29] and on nanoparticles [30], show that the vacancy formation energies strongly depend on the local positions and arrangements of the vacancy and the counterions. In a recent DFT study, for example, Migani et al. demonstrated that vacancy formation energies strongly vary for different sizes and sites on ceria nanoparticles. For the fully oxidized nanoparticles this implies that oxygen release may become very easy; however, with increasing degree of reduction, the vacancy formation energies will increase rapidly. There are two consequences that should arise from this picture: First, we would expect that the specific nanostructure of the ceria support will have an important influence on the efficiency of CO_2-induced reoxidation. Second, reoxidation by CO_2 would only be energetically possible starting from a certain minimum level of reduction. The latter idea is actually in perfect agreement with the present findings, which show that reoxidation by CO_2 is fast only on a strongly reduced surface. At moderate levels of reduction the reaction probability rapidly decreases and, finally, becomes immeasurably small, at least in the framework of our experimental approach. Concerning the detailed mechanism of CO_2-induced ceria reoxidation, we can only speculate at present. Recent XPS experiments are at least compatible with the hypothesis that CO_2 activation may involve formation of surface carboxylates, whereas the degree of carbonate formation appears not to be directly related to the reoxidation process (see [25] for details). However, further DFT calculations and model studies are required to clarify this issue fully.

In summary, we have performed a model study on the interaction of CO_2 with reduced CeO_{2-x} surfaces using a single-crystal-based model approach. Applying resonant photoelectron spectroscopy (RPES) as one of the most sensitive tools to monitor the oxidation state of ceria surfaces, we show that partial reoxidation of strongly reduced ceria occurs with high reaction probability even at temperatures as low as room temperature. In contrast to previous studies on CO_2-induced reoxidation, our experiments clearly demonstrate that (i) no noble metal component is required for CO_2 activation and decomposition on ceria and (ii) no water or OH groups are required in this process as well. In fact, CO_2 is activated on intrinsic defect sites of the surface of ceria if the concentration of Ce^{3+} centers is sufficiently high.

3. Experimental methods

The RPES measurements have been performed at the materials science beamline of the synchrotron light source Elettra in Trieste, Italy. PE spectra were acquired with a high-luminosity electron energy analyzer (Specs Phoibos 150) with 150 mm mean radius, equipped with a nine-channel detector. The experimental end station was equipped with rear-view LEED optics, a quadrupole mass spectrometer, an argon sputter gun, and a gas inlet system. The background pressure in the analysis chamber was less than 2×10^{-10} mbar during all measurements. All spectra were normalized with respect to the ring current and acquisition time. The resonant photoelectron spectra were recorded at photon energies between $h\nu = 115$ and 124.8 eV. Ce3*d*, O1*s*, and C1*s* core-level spectra were measured using Al Kα radiation, while O1*s* and C1*s* were additionally acquired using synchrotron radiation at $h\nu = 650$ and 410 eV, respectively. All spectra were acquired at constant pass energy, at emission angles of the photoelectrons with respect to the sample normal 20° and 60° (Al Kα) and 0° (synchrotron radiation). The total spectral resolutions achieved with Al Kα (1486.6 eV) and synchrotron radiation were 1 eV and 150–200 meV, respectively. The Ce3*d* core-level spectra were fitted with Voigt profiles after subtraction of a Shirley background. For the preparation of the CeO_2 film, a Cu(1 1 1) single-crystal was cleaned by several cycles of Ar^+ sputtering (at 300 K for 60 min) and annealing (723 K for 5 min) until no traces of carbon or any other contaminant was found in the photoelectron spectra. Cerium (Goodfellow, 99.99%) was evaporated at a deposition rate of 0.1 ML min^{-1} from a Mo crucible using a home-built electron-beam evaporator. During deposition the sample temperature was kept at 523 K under an oxygen partial pressure of 5×10^{-7} mbar. After Ce deposition, the film was annealed under identical conditions for 10 min. The attenuation of the Cu2*p* signal yielded a thickness of 1.8 nm, corresponding to about 6 monolayers (MLs) of ceria. Here we define 1 ML as one O–Ce–O trilayer of CeO_2(1 1 1), corresponding to a thickness of 3.13 Å. LEED measurements revealed a well-ordered CeO_2(1 1 1) film with a (1.5 × 1.5) superstructure. For details concerning the preparation procedure we refer to the literature [18–20]. For reduction, the sample was exposed to 50 L of methanol by backfilling the chamber at a sample temperature of 120 K, followed by annealing to 700 K in UHV (see [22] for details). The CO_2 (Linde, 99.995%) exposure was performed in successive doses of 1 L (1.3×10^{-8} mbar, 100 s), 10 L (5.3×10^{-8} mbar, 250 s), 200 L (5.3×10^{-7} mbar, 500 s), 4000 L (6.7×10^{-6} mbar, 800 s), 10,000 L (6.7×10^{-6} mbar, 2000 s), and 20,000 L (6.7×10^{-6} mbar, 4000 s) at 300 K by backfilling the UHV chamber.

Acknowledgments

The authors gratefully acknowledge financial support by the Deutsche Forschungsgemeinschaft (DFG) within the ERACHEM program (“NanoFunC” project), and by the Ministry of Education of the Czech Republic (LA08022). We acknowledge additional support from the DFG within the excellence cluster “Engineering of Advanced Materials” in the framework of the Excellence Initiative. We are also grateful for additional support by the Fonds der Chemischen Industrie, the DAAD (PPP, Acciones Integradas Hispano-Alemanas), and the European Union (COST D-41). Close and fruitful cooperation with M.A. Schneider, L. Hammer, H.-P. Steinrück, A. Bayer, R. Streber, and M.P.A. Lorenz (Erlangen) in the characterization of the ceria films is acknowledged.

References

[1] A. Trovarelli, Catalysis by Ceria and Related Metals, Imperial College Press, London, 2002.
[2] C. Li, Y. Sakata, T. Arai, K. Domen, K. Maruya, T. Onishi, J. Chem. Soc. Faraday Trans. I 85 (1989) 929.
[3] C. Li, Y. Sakata, T. Arai, K. Domen, K. Maruya, T. Onishi, J. Chem. Soc. Faraday Trans. I 85 (1989) 1451.
[4] L.G. Appel, J.G. Eon, M. Schmal, Catal. Lett. 56 (1998) 199–202.
[5] T. Jin, Y. Zhou, G.J. Mains, J.M. White, J. Phys. Chem. 91 (1987) 5931.
[6] S. Bernal, G. Blanco, J.M. Gatica, C. Larese, H. Vidal, J. Catal. 200 (2001) 411.
[7] O. Demoulin, M. Navez, J.L. Mugabo, P. Ruiz, Appl. Catal. B Environ. 70 (2007) 284.
[8] Y. Wang, Y. Takahashi, Y. Ohtsuka, J. Catal. 186 (1999) 160.
[9] O. Demoulin, I. Seunier, F. Dury, M. Navez, R. Rachwalik, B. Sulikowski, S.R. Gonzalez-Carrazan, E.M. Gaigneaux, P. Ruiz, Catal. Today 99 (2005) 217.
[10] R.X. Valenzuela, G. Bueno, V.C. Corberan, Y.D. Xu, C.L. Chen, Catal. Today 61 (2000) 43.
[11] H.Y. Wang, E. Ruckenstein, Appl. Catal. A Gen. 204 (2000) 143.
[12] Y.H. Hu, E. Ruckenstein, Adv. Catal. 48 (2004) 297.
[13] M.C.J. Bradford, M.A. Vannice, Catal. Rev. Sci. Eng. 41 (1999) 1.
[14] A. Bueno-Lopez, K. Krishna, M. Makkee, Appl. Catal. A Gen. 342 (2008) 144.
[15] K. Otsuka, Y. Wang, E. Sunada, I. Yamanaka, J. Catal. 175 (1998) 152.
[16] H.J. Freund, M. Baumer, J. Libuda, T. Risse, G. Rupprechter, S. Shaikhutdinov, J. Catal. 216 (2003) 223.
[17] J. Libuda, H.J. Freund, Surf. Sci. Rep. 57 (2005) 157.
[18] V. Matolín, J. Libra, I. Matolínová, V. Nehasil, L. Sedláček, F. Šutara, Appl. Surf. Sci. 254 (2007) 153.
[19] F. Šutara, M. Cabala, L. Sedláček, T. Skála, M. Škoda, V. Matolín, K.C. Prince, V. Cháb, Thin Solid Films 516 (2008) 6120.
[20] T. Staudt, Y. Lykhach, L. Hammer, M.A. Schneider, V. Matolín, J. Libuda, Surf. Sci. 603 (2009) 3382.
[21] Y. Lykhach, T. Staudt, M.P.A. Lorenz, R. Streber, A. Bayer, H.-P. Steinrück, J. Libuda, ChemPhysChem 11 (2010) 1496.
[22] V. Matolín, J. Libra, M. Škoda, N. Tsud, K.C. Prince, T. Skála, Surf. Sci. 603 (2009) 1087.
[23] T. Skála, F. Šutara, M. Škoda, K.C. Prince, V. Matolín, J. Phys. Condens. Matter 21 (2009) 0550051.
[24] A. Pfau, K.D. Schierbaum, Surf. Sci. 321 (1994) 71.
[25] Y. Lykhach, T. Staudt, R. Streber, M.P. Lorenz, A. Bayer, H.-P. Steinrück, J. Libuda, Eur. Phys. J. B 75 (2010) 89.
[26] V. Matolín, M. Cabala, V. Cháb, I. Matolínová, K.C. Prince, M. Škoda, F. Šutara, T. Skála, K. Veltruská, Surf. Interface Anal. 40 (2008) 225.
[27] V. Matolín, I. Matolínová, L. Sedláček, K.C. Prince, T. Skála, Nanotechnology 20 (2009).
[28] M. Matsumoto, K. Soda, K. Ichikawa, S. Tanaka, Y. Taguchi, K. Jouda, O. Aita, Phys. Rev. B 50 (1994) 11340.
[29] [29] M.V. Ganduglia-Pirovano, J.L.F. Da Silva, J. Sauer, Phys. Rev. Lett. 102 (2009) 026101.
[30] A. Migani, G.N. Vayssilov, S.T. Bromley, F. Illas, K.M. Neyman, Chem. Commun. 46 (2010) 5936.